Journal of Chromatography A, 1550 (2018) 21–27

Contents lists available at ScienceDirect

Journal of Chromatography A

journal homepage: www.elsevier.com/locate/chroma

O-carboxymethyl chitosan Schiff base complexes as affinity ligands for immobilized metal-ion affinity chromatography of lysozyme

Ömür Acet[a], Talat Baran[a], Demet Erdönmez[b], Neşe Hayat Aksoy[c], İhsan Alacabey[d], Ayfer Menteş[a], Mehmet Odabaşi[a,*]

[a] Aksaray University, Faculty of Arts and Science, Chemistry Department, Aksaray, Turkey
[b] Aksaray University, Faculty of Arts and Science, Biology Department, Aksaray, Turkey
[c] Aksaray University, Faculty of Veterinary Medicine, Aksaray, Turkey
[d] Mardin Artuklu University, Vocational School of Health Services, Mardin, Turkey

ARTICLE INFO

Article history:
Received 20 November 2017
Received in revised form 26 February 2018
Accepted 13 March 2018
Available online 19 March 2018

Keywords:
Cryogel
IMAC
Carboxymethyl chitosan
Lysozyme adsorption

ABSTRACT

We synthesized Ni^{2+}-attached O-Carboxymethyl chitosan Schiff base complexes embedded composite cryogels (Ni^{2+}-O-CMCS-CCs) by means of polymerization of gel-forming precursors at subzero temperatures. Prepared affinity cryogel showed excellent adsorption performance for lysozyme selected as model protein to test adsorption parameters, demonstrating an adsorption capacity of 244.6 mg/g (15.3 mg/g for Ni^{2+} minus O-CMCS-CCs), with fast adsorption equilibrium within 30 min and good reversibility. The performance of Ni^{2+}-O-CMCS-CCs for lysozyme was also evaluated by SDS-PAGE, and a purification efficiency of 86.9% with 89.5% purification yield was determined. The swelling test, FT-IR, and SEM analysis were carried out for the characterization of Ni^{2+}-O-CMCS-CCs. At the end of 35 adsorption-desorption cycles, there was no significant change in the adsorption capacity.

1. Introduction

Lysozyme (E.C. 3.2.1.17) has been extensively utilized in the pharmaceutical and nutrient industry as an anti-microbial agent and food preservative [1]. Egg white is a rich natural source of lysozyme, which composes 3–4% of the proteins in egg white [2]. Furthermore, lysozyme is utilized as an anticancer drug [3], for treatment of HIV [4], developing tumors and healing of wounds [5].

The particular separation of biomolecules is one of the most important issues in the field of biotechnology and biomedical areas [6,7]. In the last decade, immobilised metal ion affinity chromatography (IMAC) has been a commonly used technique. It is based on coordination between the chelated metal ions and functional groups of surface accessible amino acids. IMAC is handy with the laboratory medium because of its feasible conditions in order to isolate target proteins [8,9], enzymes [10], nucleic acids [11], mammalian cell culture supernatants or other biological sources [12], and bacterial toxins [13].

There are various adsorbents used for biomolecule purification with some drawbacks such as limited adsorption capacity, back pressure drop, etc [14–28]. Lately, development of composite membranes has achieved better outcomes in separation science. The composite cryogels provide some benefits such as short diffusion path, low-pressure drop, very short residence time, and a large surface area as compared with plain ones [29,30]. The small-sized particles have a large surface area, but their equipping and feasibility in separating columns present challenges. Hence, composite cryogels in which the particles are embedded into the columns can prevent further difficulties and amalgamate the positive aspects of cryogels which mentioned above [31]. Cryogels constitute of a specific group of monoliths that include polymeric, hydrophilic gels characterized by their dissimilar and supermacroporous molecular construction [32].

Chitosan has been used widely in biomedical and separation science because of its superior biocompatibility, biodegradability, non-toxicity, and adsorption features [33]. It has also plenty of functional groups (hydroxyl and amino groups) which are significant to derivatizate surface to boost adsorption capacity. It is known that the solubility of chitosan is not good. To cope with this issue and also to disperse chitosan particles regularly in the cryogel precursor solution, O-carboxymethyl chitosan Schiff base complexes were synthesized [34], and Ni^{2+} ions were combined **with** them.

* Corresponding author at: Aksaray University, Faculty of Arts and Science, Chemistry Department, Biochemistry Division, 68100 Aksaray, Turkey.
E-mail address: modabasi@aksaray.edu.tr (M. Odabaşi).

https://doi.org/10.1016/j.chroma.2018.03.022
0021-9673/

In this work, we aimed to develop a simple approach to prepare a new type and easy-to-use cryogel column embedded with Ni^{2+}-attached O-carboxymethyl chitosan Schiff base complex particles based on IMAC. The preparation and characterization of Ni^{2+}-attached O-Carboxymethyl chitosan Schiff base complexes embedded composite cryogels (Ni^{2+}-O-CMCS-CCs) columns, and the applications of these for lysozyme adsorption from aqueous solutions were investigated and discussed here, to the best of our knowledge, for the first time.

2. Methods and materials

2.1. Materials

2-Hydroxyethyl methacrylate (HEMA) was purchased from Fluka A.G (Buchs, Switzerland), *N,N′*-methylene-bis-acrylamide (MBAAm), *N,N,N′,N′*-tetramethylethylene-diamine (TEMED), and ammonium persulfate (APS) were supplied by Sigma (St. Louis, MO, USA). Lysozyme was supplied by Aldrich (Munich, Germany). All other chemicals were of reagent grade and were purchased from Merck AG (Darmstadt, Germany). Water used in the experiments was purified by using a Barnstead (Dubuque, IA, USA) ROpure LP® reverse osmosis unit.

2.2. Synthesize of O-carboxymethyl chitosan Schiff particles

We synthesized and characterized of O-carboxymethyl chitosan Schiff base in our previous study [32]. Briefly, 0.5 g of commercial chitosan was dissolved in acetic acid solution (%2, 25 mL). Then, 25 mL ethanol was added in reaction media and stirred for 1 h. A solution obtained from the reaction of 2,4-pentadione with 3-aminobenzoic acid in methanol (50 mL) was dropped into the reaction mixture and kept stirring at 60 °C for 12 h. After the Schiff base formation, 2.5 g monochloroacetic acid was added into reaction mixture and stirred for 5 days to obtain water soluble chitosan Schiff base form. After the 5 days, the product was filtered and dried at 50 °C in an oven.

2.3. Incorporation of Ni^{2+} ions to O-CMCS particles

The incorporation of Ni^{2+} ions to O-CMCS particles was carried out in 30 ppm Ni^{2+} solution (30 mL) at pH 4.7 (adjusted with 0.01 M HCl) at room temperature. The mixture was shaken with a shaker for 1 h, and the concentration of metal ions was checked by graphite furnace atomic absorption spectrometer (GFAAS, Analyst 800/Perkin Elmer, USA). The amount of chelated Ni^{2+}ions was calculated by equation (Eq. (1));

$$Q = (C_i - C_f).V/m \quad (1)$$

Where, Q is the amount of Ni^{2+} ions incorporated onto the O-CMCS particles (mg/g). C_i and C_f are the concentrations of the Ni^{2+} ions in the solution (mg/mL) before and after incorporation, respectively. V is the volume of the aqueous solution (mL), and m is the dry mass of the O-CMCS particles (g).

The leakage of Ni^{2+} ions from the Ni^{2+}-attached O-CMCS particles was researched for both pH between 4.0 and 7.0 and in a medium of 1.0 M NaCl. Ni^{2+}-attached O-CMCS particles were stirred for 24 h at room temperature, and the amount of Ni^{2+}ions in the medium was detected by an atomic absorption spectrophotometer.

2.4. Arrangement of Ni^{2+}-O-CMCS-CCs particles embedded column

The polymerization steps were briefly as follows: 2-hydroxyethyl methacrylate (HEMA, 1.75 mL) as main monomer and *N,N′*-methylene-bis-acrylamide (MBAm 40 mg) as crosslinker were dissolved in deionized water (2.2 mL), then poured into a plastic syringe with a closed outlet (5 mL, i.d. 0.8 cm). Next, 45 mg Ni^{2+}-O-CMCS was added to this mixture. Immediately after that, 100 μL of APS (10% (w/v) (as free radical producer) and 20 μL of TEMED (as catalyst) were added to prepared mixture and then incubated for 24 h at −12 °C. Afterwards, the synthesized column was brought to the room temperature and cleaned down several times with water in order to get rid of the unreacted monomers. The column was put into a fridge in buffer including 0.02% sodium azide at +4 °C until it was utilized.

2.5. Characterization studies

The swelling degree (SD) of Ni^{2+}-O-CMCS particles and Ni^{2+}-O-CMCS-CCs column were fixed in distilled water by using Eq. (2). where W_s and W_o represent the swollen and dry weight of samples, respectively. Processes for the specification of the equilibrium swelling ratio are as follows: Ni^{2+}-O-CMCS particles and composite cryogel were placed in a vacuum oven at 60 °C, then taken into distilled water to define W_o and W_s, respectively.

$$SD(\%) = (W_s - W_o)/W_o.100 \quad (2)$$

BET (Brunauer, Emmet, Teller) method was used to determine the surface area of cryogels and composites. The structural analysis of composite cryogels and O-CMCS particles were determined by the Fourier Transform Infrared (FTIR) instrument (Perkin Elmer, Spectrum 100, USA). The morphological structure of the composite cryogels and O-CMCS particles were brightened at desired magnifications by scanning electron microscopy (SEM, EVO LS 10 ZEISS 5600 SEM, Tokyo, Japan). To this end, the samples were bloated in distilled water. Afterwards, they were taken into absolute (98%) ethanol for displacement of water with alcohol molecules in the pores. After alcohol diffusion to the pores occurred, the samples were placed in an oven at nearly 60 °C to eliminate alcohol from the samples without damaging their constructions. The dehydrated samples were then covered with gold-palladium (40:60) and examined for SEM.

2.6. Lysozyme adsorption-elution studies from aqueous solutions

Lysozyme adsorption studies on composite cryogels were accomplished by using a continuous column system in accordance with certain parameters such as pH, concentration, flow rate, ionic strength, and temperature effects. The temperature effect on the system was monitored by an equipped water jacket system. The phosphate buffer of 0.05 M at pH 8.0 was applied to equilibrate the system. All studied solutions were pumped through a peristaltic pump (ALITEA, Sweden). The adsorbed amount of lysozyme was determined via UV spectrophotometer (Shimadzu, Tokyo, Japan, Model 1601) at 280 nm by comparing the initial and final lysozyme concentration of the adsorption solution. Each elution step was conducted by using 1 M NaCl at a flow rate of 1.0 mL/min for 20 min. On the other hand, the reusability of the column was determined by using 35 times with the same column. After each adsorption and elution steps, the cryogel column was washed with water and equilibrated with pH 8.0 phosphate buffer solution for the next adsorption step.

2.7. Lysozyme separation from egg white

Egg white was taken from a fresh egg, then diluted twice with phosphate buffer (20 mM, pH 8), and filtered via cheesecloth. After centrifugation of the mixture at 4 °C for 30 min at 10,000 rpm, the supernatant was evaluated for lysozyme source.

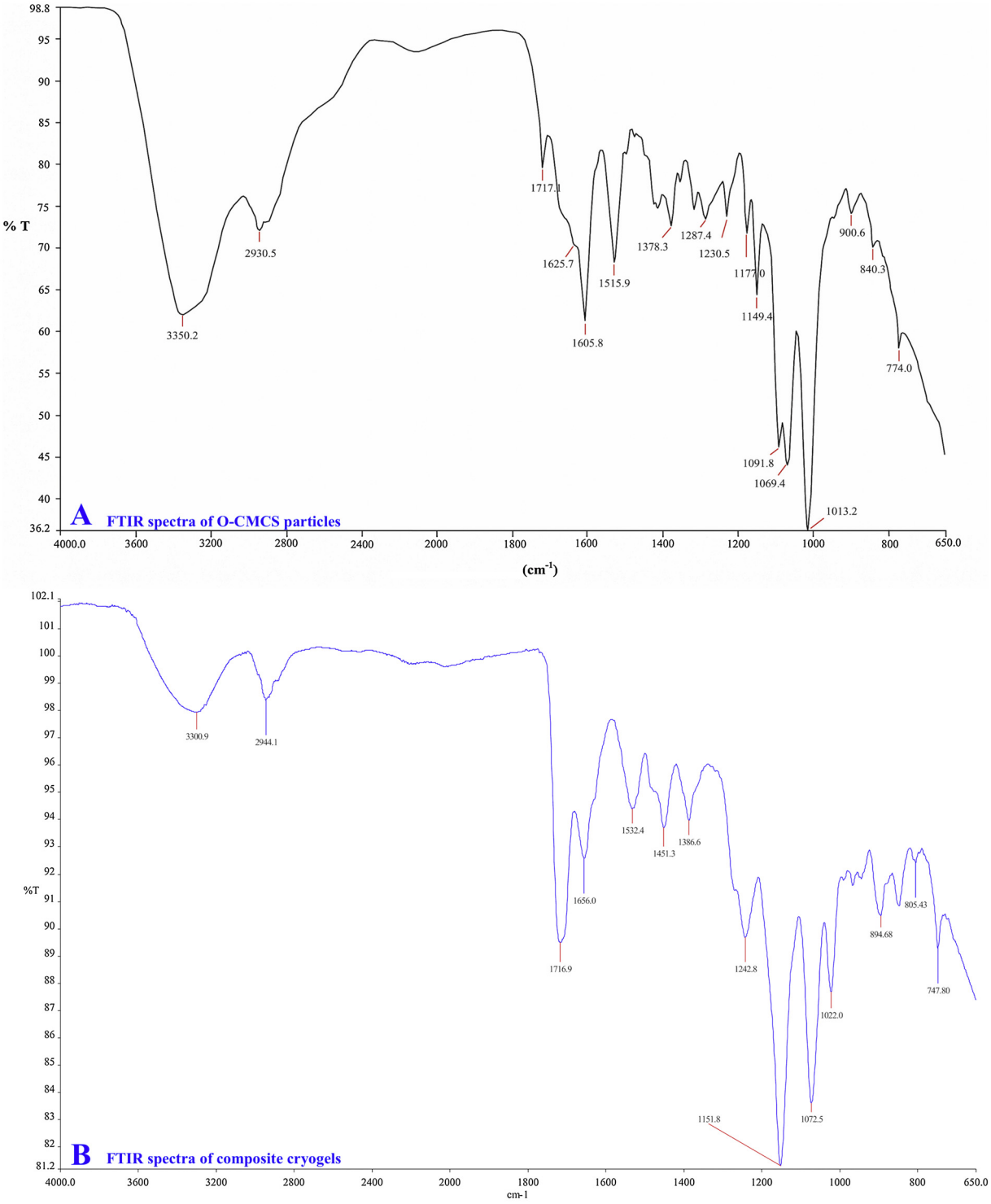

Fig. 1. The FTIR spectra of O-CMCS particles (A) and composite cryogels (B).

10 mL of this lysozyme source was passed through the column at 25 °C and a flow rate of 1 mL/min. In order to appraise column specificity for lysozyme, source solutions before and after adsorption were studied, and results were run on sodium dodecyl sulfate-polyacrylamide gel electrophoresis (SDS–PAGE) with 12% separating and 5% stacking gels. The gel was stained with Coomassie Brilliant Blue R-250, and scanned with Beckman appraise densitometer (Beckman Coulter, Appraise 4446, USA). The difference between the adsorption and desorption amount was processed for calculation of recovery yield of lysozyme from egg white solution.

3. Results and discussion

3.1. Characterization studies

The swelling ratios of O-CMCS particles and composite cryogels were determined to be 647% and 91.2%, respectively. The results

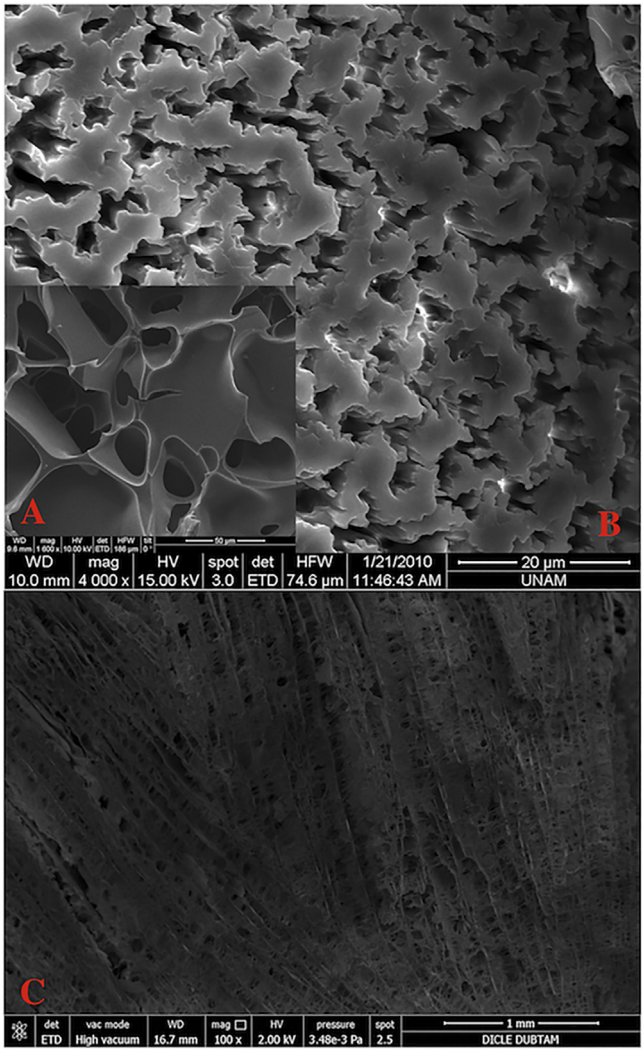

Fig. 2. SEM images of O-CMCS complexes particles (B), plain cryogel (A), and composite cryogels (C).

show that the swelling degree of plain chitosan was higher than that of the composite cryogel. The cross-linker molecules in the cryogel restricted the swelling ratio of the composite cryogel.

The amount of Ni^{2+} ions chelated on O-CMCS particles was measured as 15.6 mg/g particles. In order to research Ni^{2+} ions leaking from Ni^{2+}-attached O-CMCS particles, some experiments referred above were tested, and no leakage was found. Results showed that the washing procedure was adequate to remove the nonspecific Ni^{2+}ions attached to O-CMCS particles.

The surface area of cryogel, O-CMCS particles, and Ni^{2+}-O-CMCS-CCs were measured as 49.7, 85.4 and 76.6 m^2/g, respectively by BET method. Results showed that embedded particles were increased the surface area of composite cryogels.

FT-IR was studied for determination of the characteristic functional groups of O-CMCS particles and composite cryogels. In Fig. 1A and B, C=O stretching was shown at 1717.1 cm^{-1} and 1716.9 cm^{-1}, respectively. Also, C—N peaks at 1378.3 and 1378.0 cm^{-1} belong to O-CMCS particles and composite cryogels, respectively.

In the case of SEM images analysis, both of O-CMCS particles and composite cryogels, have greatly interconnected flow paths. Flawless macropores were shown in Fig. 2. As depicted in Fig. 2B, O-CMCS particles are composed of an indented construction with a large surface area and superb spongy structure. Even if the plain cryogels have an excellent flow rate with ideal interconnected

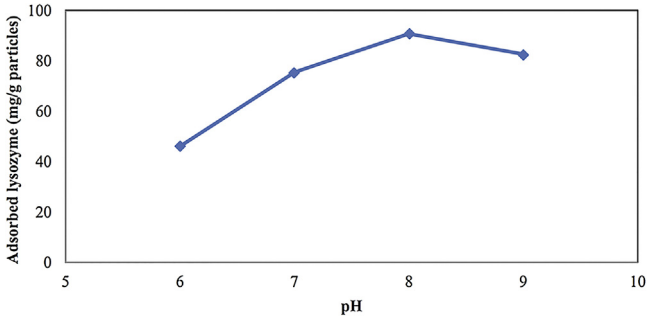

Fig. 3. Effect of pH on lysozyme adsorption onto composite cryogel, Ni^{2+}-O-CMCS particles: 45 mg; initial lysozyme concentration: 1 mg/mL; flow rate: 1 mL/min; T: 25 °C.

paths of 10–50 μm in diameter, they possess poor adsorption ability because of their low surface area (inset picture). To solve this issue of plain cryogel, these two structures were organized. As seen in Fig. 2C, O-CMCS particles were spread out uniformly into the cryogel column. It can be made inferences from Fig. 2C that composite cryogels that synthesized before have porosity of approximately 2–10 μm in diameter. There is practically no mass transfer resistance because of the size of lysozyme (27.3 Å in diameter) and high adsorption capacity because of the combination of these binary construction.

3.2. Lysozyme adsorption-elution studies from aqueous solutions

To determine the optimum conditions in adsorption studies, the factors of pH, concentration, flow rate, ionic strength, and temperature effects were examined. In the light of these results, the maximum lysozyme adsorption occurred at pH 8.0 (0.05 M phosphate buffer) (Fig. 3). The isoelectric point for lysozyme is 11.35. It inclines to cationic form at the pH values lower than the isoelectric point. In IMAC process, adsorption mainly takes place via coordination of immobilized metal ions to imidazole, indole and thiol groups of certain amino acids hanging on the protein surface [35]. Due to the deprotonation of the imidazole group around the pH 8.0, the imidazole group on the surface of lysozyme molecules interacts with immobilized metal ions.

To test the effect of initial lysozyme concentration ranging from 0.1 to 3 mg/mL on adsorption, both Ni^{2+}-O-CMCS-CCs and Ni^{2+}minus O-CMCS-CCs columns were studied to check specific and non-specific binding capacity. The highest adsorption capacity was obtained in 15 min. During this time, binding sites on the Ni^{2+}-O-CMCS-CCs column for lysozyme were satiated. No important accrual amount on adsorption occurred after the lysozyme concentration of 3 mg/mL. This status can be expressed by feeding of interaction zones on the column occupied by means of target molecules. According to Fig. 4, Ni^{2+}-O-CMCS-CCs column achieved to a high adsorption of 244.6 mg/g particles, whereas composite column without Ni^{2+} ions reached to just 15.3 mg/g particles.

To monitor the adsorption model of this study, Langmuir and Freundlich isotherm models were applied. These isotherms are the most extensively utilized isotherms to evaluate the effects of the adsorbed protein onto polymeric materials [36]. Langmuir (Eq. (3)) and Freundlich (Eq. (4)) isotherm models are given as follows, respectively:

$$\frac{C_e}{Q_e} = \frac{C_e}{Q_m} + \frac{K_d}{Q_m} \quad (3)$$

Wherein, Q_m (mg/g) is the highest adsorption at the monolayer, Ce (mg/mL) is the equilibrized concentration of lysozyme after adsorption, Q_e (mg/g) is the amount of adsorbed lysozyme per unit weight of Ni^{2+}-O-CMCS particles at equilibrium, and K_d is the dissociation

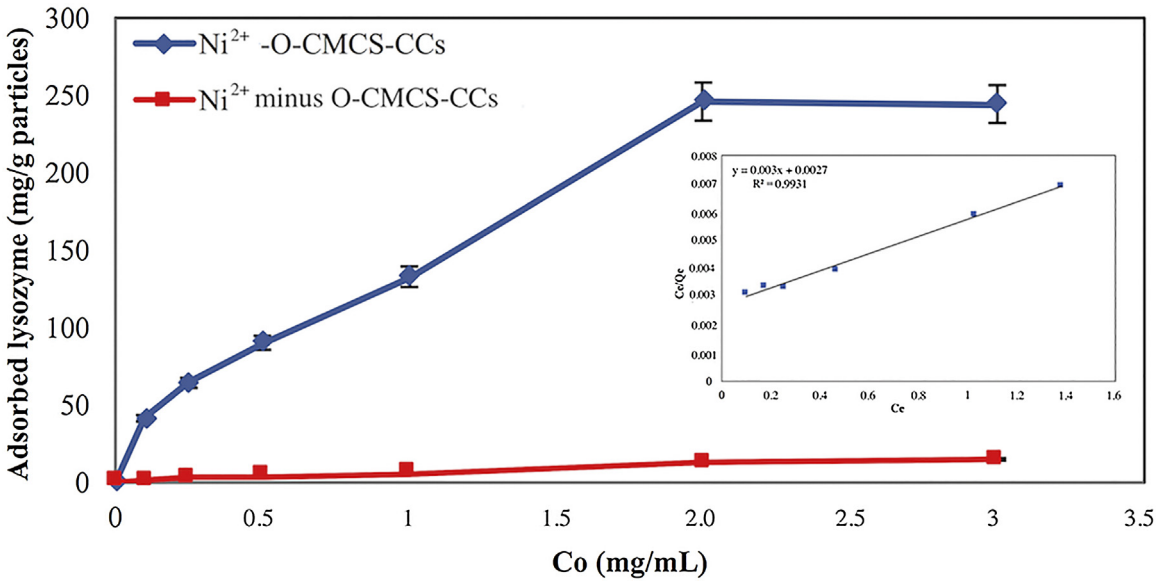

Fig. 4. Effects of initial lysozyme concentration on adsorption onto composite cryogel (The inset shows the linear representation of Langmuir equation composite cryogel), Ni^{2+}-O-CMCS particles: 45 mg; pH 8.0; flow rate: 1 mL/min; T: 25 °C.

Table 1
The parameters obtained from adsorption isotherms.

Langmuir constants			Freundlich constants		
Q_m	K_d	R^2	K_F	n	R^2
333.3	$6.1.10^{-5}$	0.999	173.6	1.2	0.971

constant of the media, which should be in the range 10^{-4}–10^{-8} M for a target molecule in an ideal adsorption system [13]

$$lnQ_e = \frac{1}{n} lnC_e + lnK_F \quad (4)$$

Here, the K_f and n present the Freundlich adsorption isotherm constants. The adsorption and the correlation coefficients of both adsorption isotherms were offered in Table 1. It can be seen from the table, according to the study data gathered, the relevance of the Langmuir adsorption isotherm is higher, and the adsorption was come true at monolayer and uniformly. The K_d value was found to be 6.1×10^{-5} M, so it can be said that the prepared composite cryogel has an ideal adsorption system.

Another important parameter, which has an influence upon protein adsorption performance is the flow rate. For this purpose, the adsorption studies were investigated in the range of between 0.5 and 3 mL/min. The highest adsorption was obtained at a flow rate of 0.5 mL/min (Fig. 5). The increase of flow velocity caused a decrease in adsorption. With ascending of flow rate, interaction time is shorter between protein and ligand. Therefore, lysozyme molecules have no more time to come in contact with cryogel walls occupied by ligands.

The effect of ionic strength on the lysozyme adsorption was also tested at different NaCl concentrations (0–0.2 M) as shown in Fig. 6. As presented in this figure, a decrease in the adsorption capacity with increasing ionic strength was observed. This phenomenon can be explained as follows: Increasing in salt concentration of the medium created a masking effect on the functional groups on adsorbent, therefore these interactions prevented the possible electrostatic interactions between ligand and lysozyme.

To test the reusability features of the Ni^{2+}-O-CMCS-CCs column, the adsorption-desorption cycles were repeated over 35 times by utilizing the same column. There was no significant change in cryogel properties. In this experiment, more than 95% of adsorbed

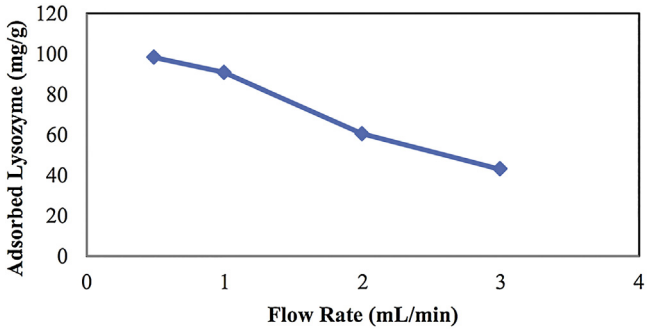

Fig. 5. Effect of flow rate on Ni^{2+}-O-CMCS particles embedded composite cryogel column; initial lysozyme concentration: 1 mg/mL, embedded Ni^{2+}-O-CMCS: 45 mg; pH 8.0; T: 25 °C.

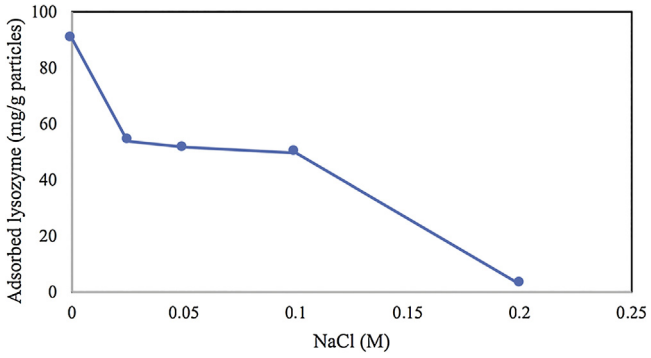

Fig. 6. Effect of ionic strength on lysozyme adsorption onto Ni^{2+}-O-CMCS particles embedded composite cryogel column, initial lysozyme concentration: 1 mg/mL; embedded Ni^{2+}-O-CMCS: 45 mg; pH 8.0; flow rate: 1 mL/min; T: 25 °C.

lysozyme was desorbed with 1 M NaCl in a short time like about 30 min. In other words, Ni^{2+}-O-CMCS-CCs column can be used over the long run.

There are many reports regarding to adsorption capacities in the literature. To compare the Ni^{2+}-O-CMCS-CCs column with other sorbents, some articles [37–42] are listed in Table 2. As seen here, among these articles, our study has a high capacity when compared

Table 2
Comparison of maximum lysozyme adsorption capacities of some sorbents in the literature.

Sorbent	Adsorption capacity (mg/g)	Ref.
Cu^{2+}-attached 3D chitin from body parts of centipede	54.1	[37]
Cu^{2+}-3D cellulose produced from trunk of *astragalus gummifer*	59.2	[38]
Efficient adsorption of hemoglobin from aqueous solutions by hybrid monolithic cryogel column	521.6	[39]
Adsorption of immunoglobulin Y in supermacroporous continuous cryogel with immobilized Cu^{2+} ions	27.7	[40]
Synthesis and performance of megaporous immobilized metal-ion affinity cryogels for recombinant protein capture and purification	12	[41]
Composite imprinted macroporous hydrogels for haemoglobin purification from cell homogenate	5.2	[42]
Protein recognition via ion-coordinated molecularly imprinted supermacroporous cryogels	22.9	[43]
Ni^{2+}-O-CMCS-CCs column	244.6	In this study

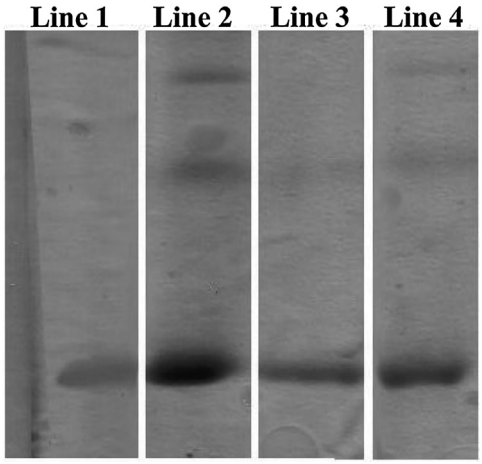

Fig. 7. Non-reducing SDS–PAGE graph. Standard lysozyme: lane 1; before and after adsorption: lane 2 and 3; desorption bands: lane 4.

with other sorbents possessing different shapes and surface functionalities. Amazing characteristics of composite cryogels emerge from composition of properties of particles (i.e., large surface area) and plain cryogels (i.e., short diffusion path, low-pressure drop etc.).

3.3. Separation of lysozyme from egg white solution

The sensitivity performance of Ni^{2+}-O-CMCS complexes embedded composite cryogels for lysozyme was evaluated via non-reducing SDS–PAGE. Fig. 7 shows the standard lysozyme, before and after adsorption as well as desorption bands are shown between lane 1 and 4, respectively.

As observed in Fig. 7, the amount of purified lysozyme is lucrative. The purification rate of lysozyme in desorption solution was computed as 86.9%. The adsorption efficiency of Ni^{2+}-O-CMCS-CCs for lysozyme was computed from the difference between before and after lysozyme adsorption amounts, and recovery yield was found as 89.5%. According to these results, it is clear that Ni^{2+}-O-CMCS complexes embedded composite cryogels can be a hope-inspiring adsorbent for purification media.

4. Concluding remarks

In this report, we discussed here a new composite column with high stability, easy preparation, good binding capability, time-saving potential, and also a low-cost cryogel matrix. Based on this point, Ni^{2+}-O-CMCS-CCs column was synthesized by free radical polymerization. Afterwards, the O-CMCS particles and composite cryogels were put through swelling tests, and the outcomes of particles and composite cryogel outputs were recorded as 697% and 91.2%, respectively. The SEM images confirmed that the prepared composite cryogel has a structure with intensive pores. These interconnected and flawless macroporous structures were provide for dynamic flow rate. The highest adsorption was observed at pH 8.0 (244.6 mg/g particles). The reusability tests verified 35 adsorption-desorption cycles in the presence of 1 M NaCl for about 30 min by utilizing the same column. Langmuir and Freundlich isotherm models for lysozyme adsorption on Ni^{2+}-O-CMCS-CCs column were utilized to determine isotherm character. The results show that the interaction behavior between the cryogel and lysozyme adheres to the Langmuir adsorption model. Thus, lysozyme molecules were adsorbed by Ni^{2+}-O-CMCS-CCs cryogels in a single homogenous fold. To conclude, this prepared composite column has potential for convenient use in the purification of lysozyme.

Acknowledgment

This study was supported by Aksaray University Scientific Research Projects Coordination (Project Number: 2015-80), Turkey.

References

[1] G. Baydemir, M. Andaç, A. Derazshamshir, D.A. Uygun, E. Özçalışkan, S. Akgöl, A. Denizli, Synthesis and characterization of amino acid containing Cu (II) chelated nanoparticles for lysozyme adsorption, Mater. Sci. Eng. C 33 (2013) 532–536.
[2] E. Abeyrathne, H. Lee, D. Ahn, Egg white proteins and their potential use in food processing or as nutraceutical and pharmaceutical agents-a review, Poult. Sci. 92 (2013) 3292–3299.
[3] D.A. Uygun, A.A. Karagözler, S. Akgöl, A. Denizli, Magnetic hydrophobic affinity nanobeads for lysozyme separation, Mater. Sci. Eng. C 29 (2009) 2165–2173.
[4] J. Ye, C. Wang, X. Chen, S. Guo, M. Sun, Marine lysozyme from a marine bacterium that inhibits angiogenesis and tumor growth, Appl. Microbiol. Biotechnol. 77 (2008) 1261–1267.
[5] V.K. Juneja, H.P. Dwivedi, X. Yan, Novel natural food antimicrobials, Annu. Rev. Food Sci. Technol. 3 (2012) 381–403.
[6] H. Aboul-Enein, I. Ali, Nano Chromatography and Capillary Electrophoresis: Pharmaceutical and Environmental Analyses, Wiley VCH, 2011.
[7] H.Y. Aboul-Enein, I. Ali, Determination of tadalafil in pharmaceutical preparation by HPLC using monolithic silica column, Talanta 65 (2005) 276–280.
[8] M. Odabaşi, R. Say, A. Denizli, Molecular imprinted particles for lysozyme purification, Mater. Sci. Eng. C 27 (2007) 90–99.
[9] M. Odabaşi, B. Garipcan, A. Denizli, Preparation of a novel metal-chelate affinity beads for albumin isolation from human plasma, J. Appl. Polym. Sci. 90 (2003) 2840–2847.
[10] H. Yavuz, M. Odabaşi, S. Akgöl, A. Denizli, Immobilized metal affinity beads for ferritin adsorption, J. Biomater. Sci. Polym. Ed. 16 (2005) 673–684.
[11] M. Odabaşı, G. Baydemir, M. Karataş, A. Derazshamshir, Preparation and characterization of metal-chelated poly (HEMA-MAH) monolithic cryogels and their use for DNA adsorption, J. Appl. Polym. Sci. 116 (2010) 1306–1312.

[12] J.T. Mooney, D.P. Fredericks, C. Zhang, T. Christensen, C. Jespergaard, C.B. Schiødt, M.T. Hearn, Purification of a recombinant human growth hormone by an integrated IMAC procedure, Protein Expr. Purif. 94 (2014) 85–94.
[13] F. Gurbuz, Ş. Ceylan, M. Odabaşı, G.A. Codd, Hepatotoxic microcystin removal using pumice embedded monolithic composite cryogel as an alternative water treatment method, Water Res. 90 (2016) 337–343.
[14] I. Ali, Z.A. Alothman, A. Alwarthan, Uptake of propranolol on ionic liquid iron nanocomposite adsorbent: kinetic, thermodynamics and mechanism of adsorption, J. Mol. Liq. 236 (2017) 205–213.
[15] I. Ali, Z.A. AL-Othman, A. Alwarthan, Molecular uptake of congo red dye from water on iron composite nano particles, J. Mol. Liq. 224 (2016) 171–176.
[16] I. Ali, Z.A. AL-Othman, A. Alwarthan, Green synthesis of functionalized iron nano particles and molecular liquid phase adsorption of ametryn from water, J. Mol. Liq. 221 (2016) 1168–1174.
[17] I. Ali, Z.A. AL-Othman, A. Alwarthan, Synthesis of composite iron nano adsorbent and removal of ibuprofen drug residue from water, J. Mol. Liq. 219 (2016) 858–864.
[18] I. Ali, Z.A. Al-Othman, O.M. Alharbi, Uptake of pantoprazole drug residue from water using novel synthesized composite iron nano adsorbent, J. Mol. Liq. 218 (2016) 465–472.
[19] S. SHARMA, A. Imran, Adsorption of Rhodamine B dye from aqueous solution onto acid activated mango (Magnifera indica) leaf powder: equilibrium, kinetic and thermodynamic studies, J. Toxicol. Environ. Health Sci. 3 (2011) 286–297.
[20] I. Ali, V.K. Gupta, T.A. Khan, M. Asim, Removal of arsenate from aqueous solution by electro-coagulation method using Al-Fe electrodes, Int. J. Electrochem. Sci. 7 (2012) 1898–1907.
[21] I. Ali, Z.A. Alothman, A. Alwarthan, Supra molecular mechanism of the removal of 17-β-estradiol endocrine disturbing pollutant from water on functionalized iron nano particles, J. Mol. Liq. 241 (2017) 123–129.
[22] I. Ali, C.K. Jain, Advances in arsenic speciation techniques, Int. J. Environ. Anal. Chem. 84 (2004) 947–964.
[23] I. Ali, T.A. Khan, M. Asim, Removal of arsenate from groundwater by electrocoagulation method, Environ. Sci. Pollut. Res. 19 (2012) 1668–1676.
[24] I. Ali, Z.A. Al-Othman, A. Alwarthan, M. Asim, T.A. Khan, Removal of arsenic species from water by batch and column operations on bagasse fly ash, Environ. Sci. Pollut. Res. 21 (2014) 3218–3229.
[25] I. Ali, Z.A.A.L. Othman, M.M. Sanagi, Green synthesis of iron nano-impregnated adsorbent for fast removal of fluoride from water, J. Mol. Liq. 211 (2015) 457–465.
[26] I. Ali, Z.A.L. Othman, A. Al-Warthan, Sorption, kinetics and thermodynamics studies of atrazine herbicide removal from water using iron nano-composite material, Int. J. Environ. Sci. Technol. (Tehran) 13 (2016) 733–742.
[27] I. Ali, Z.A. Al-Othman, A. Al-Warthan, Removal of secbumeton herbicide from water on composite nanoadsorbent, Desalin. Water Treat. 57 (2016) 10409–10421.
[28] M.H. Dehghani, D. Sanaei, I. Ali, A. Bhatnagar, Removal of chromium (VI) from aqueous solution using treated waste newspaper as a low-cost adsorbent: kinetic modeling and isotherm studies, J. Mol. Liq. 215 (2016) 671–679.
[29] C. Wang, X.-Y. Dong, Z. Jiang, Y. Sun, Enhanced adsorption capacity of cryogel bed by incorporating polymeric resin particles, J. Chromatogr. A 1272 (2013) 20–25.
[30] M. Erzengin, N. Ünlü, M. Odabaşı, A novel adsorbent for protein chromatography: supermacroporous monolithic cryogel embedded with Cu 2+-attached sporopollenin particles, J. Chromatogr. A 1218 (2011) 484–490.
[31] Ş.C. Cömert, M. Odabaşı, Investigation of lysozyme adsorption performance of Cu^{2+}-attached PHEMA beads embedded cryogel membranes, Mater. Sci. Eng. C 34 (2014) 1–8.
[32] M. Bakhshpour, A. Derazshamshir, N. Bereli, A. Elkak, A. Denizli, [PHEMA/PEI]–Cu (II) based immobilized metal affinity chromatography cryogels: application on the separation of IgG from human plasma, Mater. Sci. Eng. C 61 (2016) 824–831.
[33] N. Kathuria, A. Tripathi, K.K. Kar, A. Kumar, Synthesis and characterization of elastic and macroporous chitosan–gelatin cryogels for tissue engineering, Acta Biomater. 5 (2009) 406–418.
[34] T. Baran, A. Menteş, H. Arslan, Synthesis and characterization of water soluble O-carboxymethyl chitosan Schiff bases and Cu (II) complexes, Int. J. Biol. Macromol. 72 (2015) 94–103.
[35] A. Derazshamshir, B. Ergün, G. Peşint, M. Odabaşı, Preparation of Zn^{2+}-chelated poly (HEMA-MAH) cryogel for affinity purification of chicken egg lysozyme, J. Appl. Polym. Sci. 109 (2008) 2905–2913.
[36] M. Uygun, Dye-attached cryogels for reversible alcohol dehydrogenase immobilization, J. Chromatogr. B 959 (2014) 42–48.
[37] E. Bulut, I. Sargin, O. Arslan, M. Odabasi, B. Akyuz, M. Kaya, In situ chitin isolation from body parts of a centipede and lysozyme adsorption studies, Mater. Sci. Eng. C 70 (2017) 552–563.
[38] M. Kaya, M. Odabasi, M. Mujtaba, M. Sen, E. Bulut, B. Akyuz, Novel three-dimensional cellulose produced from trunk of Astragalus gummifer (Fabaceae) tested for protein adsorption performance, Mater. Sci. Eng. C 62 (2016) 144–151.
[39] N.Y. Baran, Ö. Acet, M. Odabaşı, Efficient adsorption of hemoglobin from aqueous solutions by hybrid monolithic cryogel column, Mater. Sci. Eng. C 73 (2017) 15–20.
[40] W.F. da Silva Júnior, R. Cano, A.H. Totola, L.M. de Carvalho, M.O. Cerri, J.S. dos Reis Coimbra, G.G.P. de Carvalho, B.M.A. de Carvalho, Adsorption of immunoglobulin Y in supermacroporous continuous cryogel with immobilized Cu^{2+} ions, J. Chromatogr. A 1395 (2015) 16–22.
[41] N.S. Bibi, N.K. Singh, R.N. Dsouza, M. Aasim, M. Fernández-Lahore, Synthesis and performance of megaporous immobilized metal-ion affinity cryogels for recombinant protein capture and purification, J. Chromatogr. A 1272 (2013) 145–149.
[42] S. Hajizadeh, K. Kettisen, M. Gram, L. Bülow, L. Ye, Composite imprinted macroporous hydrogels for Haemoglobin purification from cell homogenate, J. Chromatogr. A 1534 (2017) 22–31.
[43] N. Bereli, M. Andaç, G. Baydemir, R. Say, I.Y. Galaev, A. Denizli, Protein recognition via ion-coordinated molecularly imprinted supermacroporous cryogels, J. Chromatogr. A 1190 (2008) 18–26.